scientific reports

Check for updates

OPEN

In silico evaluation of the immunogenic profile of lung cancers with *SMARCA4* genetic alterations

Cristina Nieto-Jiménez[1,10], Esther Garcia-Lorenzo[2,10], Cristina Diaz-Tejeiro[1], Lucía Paniagua-Herranz[1], Adrián Sanvicente[1,3], Bernard Doger[2], Irene Moreno[4], Manuel Pedregal[2], Jorge Bartolomé[5], Arancha Manzano[5], Gyöngyi Munkácsy[6,7], Balázs Győrffy[6,7,8], Pedro Pérez-Segura[5], Emiliano Calvo[4], Victor Moreno[2] & Alberto Ocana[1,2,5,9]✉

Genomic alterations in tumor cells can influence immune response, as has been demonstrated in several tumor types. For instance, mutations in certain genes like EGFR or B-RAF are associated with a particular immune phenotype. Non-small cell lung cancer (NSCLC) is one of the most immunogenic tumors, but certain genomic alterations can modulate and influence immune response. In the present work, we explore the transcriptomic landscape and immunologic profile of NSCLC with molecular alterations in *SMARCA4*. Using the TCGA repository we exploited their analysis with R and other available packages. cBioPortal was used to explore and analyze the mutational profile present in those tumors The prognostic value of identified genes in patients treated with immunotherapy was evaluated using the KMplotter online tool, and for correlations with immune populations TIMER 2.0 was interrogated. In lung adenocarcinoma (LUAD) and squamous cell carcinoma (LUSC) disruptive mutations in *SMARCA4* were presented in 8%, and 4% of the cases, respectively. Gene deletions were observed in 1% of the population. The transcriptomic profile in LUAD and LUSC with deletions or disruptive mutations was explored. Interrogating TCGA using a 2.5 gene expression fold change (FC) we observed five genes commonly upregulated, and thirty-one genes commonly decreased when *SMARCA4* was mutated or CNV loss was present. Enriched biological functions for downregulated genes included "Antigen processing and presentation, endogenous lipid antigen via MHC class Ib. Expression of *CD1A*, *CD1C*, *CD1E*, *CX3CR1*, and *MYO1G* showed a strong positive correlation with dendritic cells (DC) and dendritic cells resting (DCR). The increased expression of gene signatures formed by these transcripts resulted in a better prognosis in a set of patients with different tumors treated with anti-PD1 therapies, including 21 non-small cell lung cancers. We evaluated genomic alterations and transcriptomic patterns of *SMARCA4* alterations in NSCLC tumors, identifying a relevant immunologic downregulated gene set linked with antigen presentation that predicts response to anti-PD1 therapies.

Keywords Lung adenocarcinoma, LUAD, *SMARCA4*, Immune response, Immunologic profile

[1]Experimental Therapeutics Unit, Hospital Clínico San Carlos (HCSC) Instituto de Investigación Sanitaria San Carlos (IdISSC), Madrid, Spain. [2]START Madrid-FJD, Hospital Fundación Jiménez Díaz, Madrid, Spain. [3]Facultad Ciencias Químicas, Universidad Complutense, Madrid, Spain. [4]START Madrid-CIOCC, Centro Integral Oncológico Clara Campal, Madrid, Spain. [5]San Carlos Clinical Hospital, Oncology, Madrid, Spain. [6]Department of Bioinformatics, Semmelweis University, Tűzoltó U. 7-9, Budapest 1094, Hungary. [7]Research Centre for Natural Sciences, Hungarian Research Network, Magyar Tudosok Korutja 2, Budapest 1117, Hungary. [8]Department of Biophysics, Medical School, University of Pecs, Pecs 7624, Hungary. [9]Breast Cancer, Centro de Investigación Biomédica en Red en Oncología (CIBERONC), Madrid, Spain. [10]Cristina Nieto-Jiménez and Esther Garcia-Lorenzo contributed equally to this work. ✉email: alberto.ocana@salud.madrid.org

Immunotherapy has gained momentum with the approval of several agents, in different indications, demonstrating a clear improvement in time-to-event endpoints like progression-free survival (PFS) or overall survival (OS)[1]. However, it has become clear that not all patients respond to this treatment and, for some of them, response durations are limited in time, suggesting the importance of identifying biomarkers of response[1,2]. Two kinds of biomarkers have been developed and incorporated in the clinical setting: those related to the expression of the target ligand (PD-L1); and those associated with the genomic profile of the tumor itself, including MSI-H / D-MMR or high tumor mutational burden (TMB)[2]. Other explored biomarkers include tumor microenvironment (TME) factors, such as the presence of tumor-infiltrating lymphocytes (TILs), gene expression signatures, or tumor molecular profiles[2]. In recent years, much of the research in this field has focused on the identification of biological alterations that could be used as surrogate markers of activity, or targets for the development of novel immune checkpoint inhibitors (ICIs)[1,2].

Non-small cell lung cancer (NSCLC) is one of the most sensitive tumors to ICI[3]. Currently, immunotherapy alone or in combination with chemotherapy in NSCLC, without molecular driver alterations, is the treatment of choice in first line[2,3]. However, while elevated PD-L1 expression has been associated with increased response to ICIs, it has also been shown that patients with PD-L1-positive tumors may not respond, and patients with PD-L1-negative tumors may experience clinical benefit, demonstrating the complexity of the biological scenario, and the necessity to identify better biomarkers for patient selection[2,4]. Given the current experience, other biomarkers beyond PD-L1 could affect the clinical activity of ICI. For instance, genomic alterations within the tumor can influence the immune microenvironment[4].

How driver mutations change the immune response has been studied in some situations. For example, tumors with mutations in druggable genes like *EGFR, ALK,* or *ROS* are known to experience a worse response to immunotherapy[2,4]. On the other hand, little information about the immune microenvironment and the tumoral presence of mutations at BRAF, *RET,* or *MET* has been reported[3]. In a similar way, limited data has been reported in relation with *SMARCA4* alterations and immune response. However, a recent article associates *SMARCA4* loss with decreased response to anti-PD1 immunotherapy, which tumors were associated with significantly low infiltration of dendritic cells (DCs) and CD4 + T cells into the tumor microenvironment (TME)[5].

SMARCA4 is a gene located on chromosome 19p13 that encodes the expression of the BRG1 transcription activator, one of the most common abnormal ATP-dependent catalytic subunits of the SWI/SNF chromatin remodeling complex[6,7]. *SMARCA4* is a tumor suppressor gene mutation that contributes to tumorigenesis. Loss of function mutations in *SMARCA4* lead to disruption of chromatin regulation, promoting uncontrolled cell proliferation[6,7]. *SMARCA4* has several functions, including the regulation of gene expression, differentiation, and transcription, which justifies why its mutation, especially homozygous deletions, and truncations, has been associated with a weak response to conventional chemotherapy and poor prognosis in tumors like lung adenocarcinoma (LUAD)[6,7]. In line with this, the 2021 WHO Classification of Lung Tumors (fifth edition) recognized thoracic *SMARCA4*-deficient undifferentiated tumor as a new lung cancer subtype. NSCLC with no expression of *SMARCA4* is currently understood as *SMARCA4*-negative adenocarcinoma, *SMARCA4*-negative squamous cell carcinoma, or thoracic *SMARCA4*-deficient undifferentiated tumor[8].

SMARCA4 alterations are divided into class I mutations (loss of function) such as truncations, fusions, and deletions, and class II, which are nonsense mutations or variants of unknown significance[6]. Although class II are the most frequent *SMARCA4* alterations, class I mutations are predominant in *SMARCA4* mutated NSCLC[6]. In line with this, only loss of *SMARCA4* function have been associated with a lack of activity to anti-PD1 therapies[5].

Given the influence that genomic changes have on the immune microenvironment and how this can influence the respond against immune-check point inhibitors, in this work we aimed to evaluate the immunogenic profile of lung cancers with *SMARCA4* genetic alterations.

Material and methods

Data collection and processing

Data from TCGA was downloaded to evaluate the expression of transcripts up or downregulated when deletions or disruptive mutations of *SMARCA4* were present in LUAD. Supplementary table 1 summarized the studies selected for the analysis.

Genomic alteration and transcriptomic analysis

Information from mutations was extracted from the TCGA Lung adenocarcinoma Pan-cancer atlas study contained at CBioPortal (http://www.cbioportal.org)[9]. This database contains 507 samples with mutation and copy number alterations (CNA). CBioPortal was used to identify and classify mutations in *SMARCA4* in lung adenocarcinoma samples. CBioPortal classifies mutations into driver (mutations that may be linked to oncogenesis) or VUS (variant of unknown significance). VUS mutations are those that have not been studied by the OncoKB team and their relevance in the tumor is unknown. Structural variation is defined as a region of DNA that can include inversions and balanced translocations or genomic imbalances. Deep deletion indicates a deep loss, possibly a homozygous deletion. Amplification indicates a high-level amplification (more copies, often focal). Mutations are changes in DNA sequences. Disruptive mutations are defined as mutations that result in a disrupted protein structure.

Information for patient outcomes including overall survival (OS) and disease-free progression (DFP) of patients was analyzed depending on whether they had altered *SMARCA4* or not.

Transcriptomic information was also extracted from TCGA mapping including genes that were upregulated when *SMARCA4* had disruptive mutations and upregulated when gene deletion was present. For this comparison among genes, we used a fold change greater than 2.5, for both conditions upregulated and downregulated.

For graphical representations we used http://bioinformatics.psb.ugent.be/webtools/Venn/.

Gene set enrichment analysis

Selected mutated genes were analyzed using the g.profiler biological functional enrichment analysis tool (https://biit.cs.ut.ee/gprofiler/gost) (accessed in January 2025). The highlighted GO molecular function terms were selected. These terms are calculated using a greedy search strategy that recalculates the hypergeometric p-values with new parameters. This approach ensures that several principal terms of a component are taken into account, rather than simply selecting the term with the highest level of significance. For the smallest group of genes, an individualized search of each gene was performed in GeneCards (https://www.genecards.org/) (accessed in August 2023), and its biological function was detailed.

Correlation between gene expression and immune cell infiltration

Tumor Immune Estimation Resource (TIMER 2.0) was used to explore the associations between gene expression and immune infiltration cells (http://timer.cistrome.org/, last time accessed on February 2024)[10]. TIMER provides 4 modules (Gene, Mutation, sCNA, and Outcome) to explore the association between immune infiltrates (such as CD8 + and CD4 + ; T cells; B cells and neutrophils, among others, in LUAD) and their genomic changes[10]. The gene module (Immune association) was used to link gene expression with dendritic cell population.

Outcome analyses

The KM Plotter, as described in http://www.kmplot.com[11] correlates gene expression of the identified transcripts with clinical outcome of patients treated with immunotherapy. Datasets used in this analysis were indicated in Szonja Anna Kovácshttps et al.[12].

Results

Structural genomic alterations of SMARCA4 in lung adenocarcinomas

We first explored the frequency of molecular alterations of *SMARCA4* in different tumors as displayed in Supplementary Fig. 1 (data from TCGA-Pan cancer atlas). Tumors with the highest number of alterations included endometrial, melanoma, and esophageal followed by ovarian, lung adenocarcinoma, and stomach.

In this work, we focused on non-small cell lung cancer (NSCLC), where the percentage of squamous lung cancer (LUSC) and adenocarcinoma (LUAD) patients with *SMARCA4* mutations were analyzed. In LUAD, 43 out of 507 (8.48%) evaluated patients presented disruptive mutations, and 5 and 2 out of 507 (0.98–0.39%) for gene deletions and structural variants, respectively (Fig. 1A). In LUSC, the proportion was smaller with 17 out of 466 patients analyzed (3.65%) and 3 out of 466 with gene deletions (0.64%) (Fig. 1A).

Taking into consideration the 50 *SMARCA4* mutations in all LUAD cancer patients analyzed, 27 were defined as driver mutations: 15 as truncating, 6 as splicing, 2 as fusion, and 4 as missenses. From variants of uncertain significance (VUS) mutations, all of them were missense mutations (Fig. 1B). In LUSC, 13 out of 21 *SMARCA4* mutations were considered driver mutations, of which most were truncating (Fig. 1B).

Figure 1C displays the arrangement of mutations along the *SMARCA4* gene in LUAD and LUSC, and the type of mutation as indicated in the legend. In this diagram, the Y-axis indicates the number of patients with each mutation. The diagram represents the structure of the gene, with the location of its most prominent domains, and the position where the mutations are located (the X-axis shows the number of amino acids). As we can see, the missense mutations are the most frequent in the population and are located along the entire gene.

When evaluating the outcome, both overall survival (OS) and progression-free survival (PFS) in *SMARCA4* mutated tumors had shorter survival in LUAD, as displayed in Fig. 1D. In LUSC, *SMARCA4*-mutated tumors had no worse overall survival or progression-free survival (Fig. 1E).

Co-occurring mutations in lung adenocarcinomas with mutated SMARCA4

We next explored the co-occurrence of mutations in *SMARCA4* mutated NSCLC. To do so, we selected those genes that were mutated in at least 15% of patients using data from TCGA as described in material and methods (Fig. 2A). We obtained a list of 10 genes that showed co-occurrence with *SMARCA4* in LUAD with at least 3% frequency (Fig. 2B). These transcripts included *TTN, RYR2, USH2A, PTPRD, COL11A1, KEAP1, RYR3, NRXN1, FAT4* and *SI*.

To better understand the function of these genes, we performed a functional enrichment analysis using as described in the methodology. Most of the genes that showed a co-occurrence with *SMARCA4* were involved in calcium-related pathways (*RYR2, RYR3, TTN, NRXN1,* and *FAT4*), response to mechanical stimuli (*TTN, RYR2, COL11A1,* and *NRXN1*), or adhesion (*PTRPD, NRXN1,* and *FAT4*) (Fig. 2C). The functions shown in the graph were the most relevant terms identified.

In parallel, we analyzed those genes that co-occur with *SMARCA4* mutations from the whole spectrum of genes, independently of the mutational frequency; and selected those in which both mutations were present in at least 10 out of the total of 565 patients (Fig. 3A). Most frequent include genes included *RYR2, USH2A, SPTA1, COL11A1, PCDH15, FAT4, RYR3, FBN2, COL3A1* among others. We note that many of the functions and genes were similar to the previous ones, with the addition of some functions such as cell differentiation (*USH2A, SPTA1, COL11A1, PCDH15, FAT4, FBN2, COL3A1, VCAN, HCN1, ADGRB3, SLC39A12, NLRP14, SPEF2, COL12A1, NLRP3, SALL1, ABCB5, HECW1* and *CTNNA2*), or neuron generation (*USH2A, PCDH15. FAT4, COL3A1, VCAN, HCN1, ADGRB3, SLC39A12, SALL1, HECW1* and *CTNNA2*) (Fig. 3B).

Transcriptomic profile of tumors with mutations or CNV loss

We next explored the transcriptomic profile (upregulated and downregulated gene sets) when *SMARCA4* was mutated or when CNV loss was present. Using a 2.5 gene expression fold change (FC) we observed 48 genes that were upregulated and 428 genes that were downregulated in tumors with disruptive mutations in *SMARCA4*; and 80 upregulated and 186 downregulated genes when *SMARCA4* deletions were present (Fig. 4A).

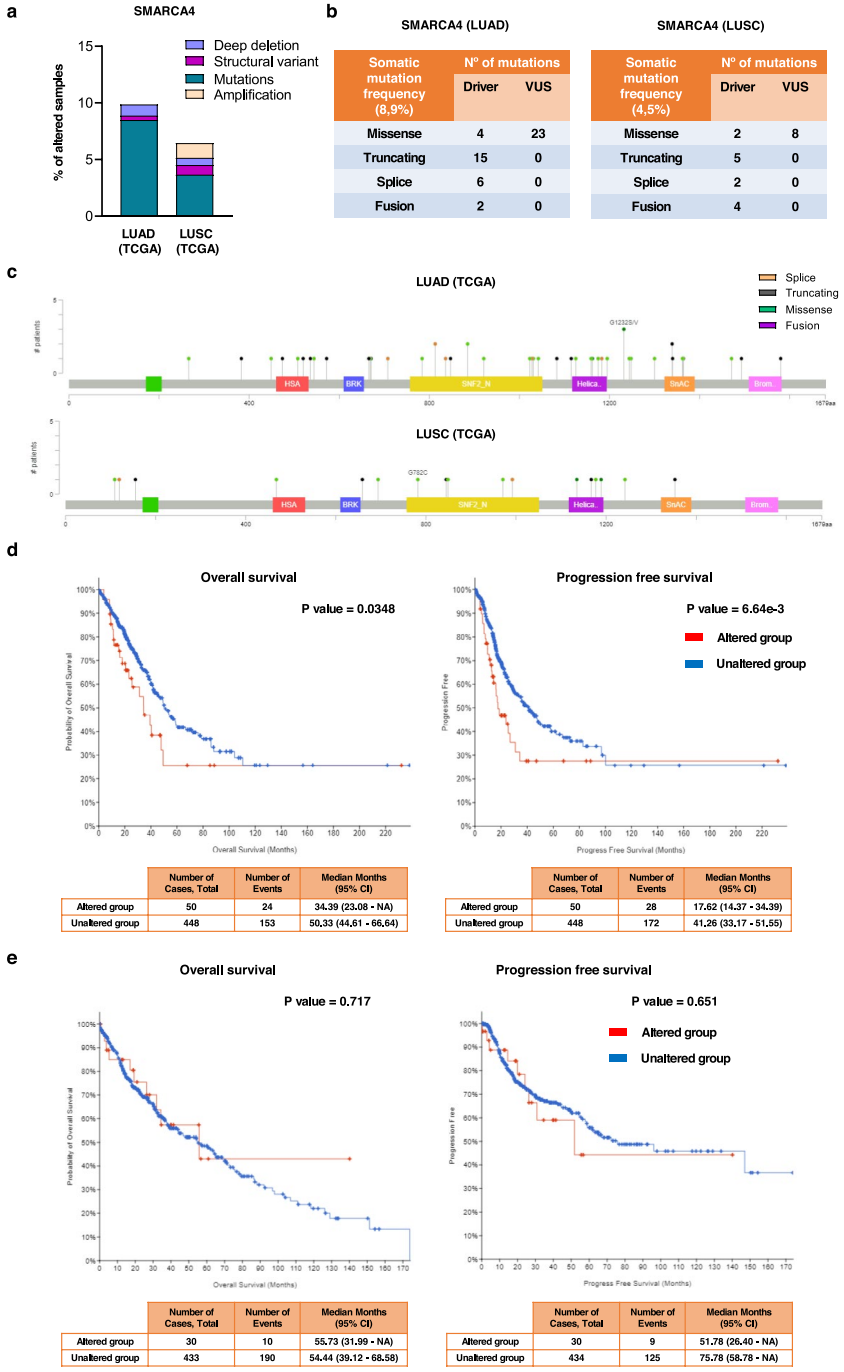

Fig. 1. Structural genomic alterations of *SMARCA4* in LUAD (566 samples) and LUSC (487 samples). (**A**) Percentage of LUAD and LUSC samples altered in *SMARCA4* and type of alteration. (**B**) Somatic driver or VUS mutation frequency. Within each group of mutations were subclassified into fusions, splices, missense, and truncating. (**C**) Maps mutations of *SMARCA4* on a linear protein and its domains (lollipop plots). (**D**) Kaplan–Meier survival curves that evaluate overall survival and progression-free survival when *SMARCA4* was altered in LUAD. (**E**) Kaplan–Meier survival curves that evaluate overall survival and progression-free survival when *SMARCA4* was altered in LUSC.

Next, we compared upregulated or downregulated genes that were shared between both conditions (disruptive mutations and CNV loss). Among the genes that were overexpressed, we found five common genes: *PKD1L2, S100P, OSGIN1, NMRAL2P,* and *TXNRD1* (Fig. 4B). Common genes downregulated when *SMARCA4* was mutated or CNV loss were present included thirty-one, as indicated in Fig. 4B.

a

Gene	Freq
TP53	52,10%
TTN	48,10%
MUC16	42,80%
CSMD3	39,90%
RYR2	38,30%
LRP1B	35,50%
ZFHX4	32,70%
USH2A	31,30%
KRAS	29,70%
XIRP2	26,50%
SPTA1	26,10%
FLG	25,60%
CSMD1	22,10%
NAV3	21,70%
FAT3	21,40%
COL11A1	21,20%
PCDH15	20,80%
ZNF536	20,70%
MUC17	19,60%
ANK2	19,60%
PCLO	19,30%
RYR3	18,70%
APOB	18,40%
KEAP1	18,00%
PAPPA2	17,80%
DNAH9	17,50%
ADAMTS12	17,50%
ADGRG4	17,30%
RP1L1	17,10%
RYR1	16,80%
TNR	16,80%
FBN2	16,60%
SI	16,40%
CDH10	16,30%
PTPRD	16,30%
NRXN1	16,30%
HMCN1	16,10%
CACNA1E	15,90%
ABCA13	15,50%
ZNF804A	15,50%
NPAP1	15,40%
DMD	15,40%
ERICH3	15,40%
PCDH11X	15,20%
FAM135B	15,20%
FAT4	15,20%
RELN	15,20%
PXDNL	15,20%
NALCN	15,00%

b

A	B	Neither	A Not B	B Not A	Both	q-Value	Freq %
TTN	*SMARCA4*	244	213	16	34	0.006	6,71
RYR2	*SMARCA4*	286	171	21	29	0.008	5,72
USH2A	*SMARCA4*	306	151	25	25	0.024	4,93
PTPRD	*SMARCA4*	355	102	30	20	0.011	3,94
COL11A1	*SMARCA4*	364	93	31	19	0.009	3,75
KEAP1	*SMARCA4*	375	82	33	17	0.017	3,35
RYR3	*SMARCA4*	366	91	33	17	0.035	3,35
NRXN1	*SMARCA4*	389	68	34	16	0.006	3,16
FAT4	*SMARCA4*	396	61	35	15	0.008	2,96
SI	*SMARCA4*	382	75	35	15	0.036	2,96

c

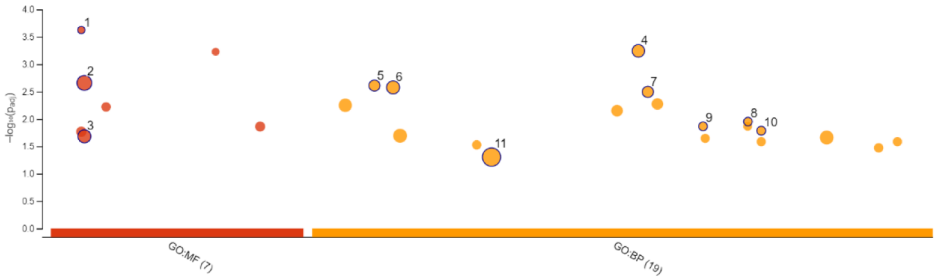

Source	Function	Term_id	Adjusted pvalue	Genes
GO:MF	1. Ryanodine-sensitive calcium-release channel activity	GO:0005219	2,37E-04	*RYR2; RYR3*
GO:MF	2. Calcium ion binding	GO:0005509	2,19E-03	*TTN; RYR2; RYR3; NRXN1; FAT4*
GO:MF	3. Calmodulin binding	GO:0005516	2,08E-02	*TTN; RYR2; RYR3*
GO:BP	4. Response to calcium ion	GO:0051592	5,70E-04	*TTN; RYR2; RYR3; NRXN1*
GO:BP	5. Heterophilic cell-cell adhesion via plasma membrane cell adhesion molecules	GO:0007157	2,45E-03	*PTPRD; NRXN1, FAT4*
GO:BP	6. Response to mechanical stimulus	GO:0009612	2,65E-03	*TTN; RYR2; COL11A1; NRXN1*
GO:BP	7. Cardiac muscle tissue morphogenesis	GO:0055008	3,19E-03	*TTN; RYR2; COL11A1*
GO:BP	8. Presynaptic membrane assembly	GO:0097105	1,12E-02	*PTPRD; NRXN1*
GO:BP	9. Cellular response to caffeine	GO:0071313	1,36E-02	*RYR2; RYR3*
GO:BP	10. Regulation of postsynaptic density assembly	GO:0099151	1,64E-02	*PTPRD; NRXN1*
GO:BP	11. Multicellular organismal process	GO:0032501	4,96E-02	*TTN; RYR2; USH2A; PTPRD; COL11A1; KEAP1; RYR3; NRXN1; FAT4; SI*

Fig. 2. Co-occurring mutational status of *SMARCA4* with the most altered genes in LUAD. (**A**) List of genes with more than 15% mutation frequency in LUAD (CBioPortal). (**B**) Genes showing co-occurrence with *SMARCA4* in LUAD. Those samples that are mutated for the most frequent genes (**A**), for *SMARCA4* (**B**), for both genes (Both) and those that are mutated in neither (Neither) are indicated. The frequency was calculated with the number of samples with both mutated genes referenced to the total number of samples. (**C**) Functional enrichment analysis using the g.profiler web tool. This tool provides us with a map of the functions in which the *p* value of each function was reflected and the size of the circle depends on the number of genes involved in each one. We selected those functions that the software itself indicates as relevant to the function cluster GO molecular function or biological processes.

Gene-set enrichment analysis

Next, we evaluated molecular and biological functions related to the gene sets identified for both conditions. For those transcripts that were upregulated, due to the low number of common genes, we used the GeneCards[13]. As can be seen in Supplementary Table 2, these genes are grouped into a wide range of different functions.

a

Gene	p value	Both genes mutated
RYR2	5,24E-04	28
USH2A	4,01E-03	23
SPTA1	6,88E-03	19
COL11A1	3,33E-03	17
PCDH15	4,43E-03	16
FAT4	1,25E-03	15
RYR3	7,66E-03	15
FBN2	1,90E-03	14
COL3A1	2,95E-05	13
VCAN	2,40E-03	13
HCN1	7,30E-05	12
CUBN	6,75E-04	12
ADGRB3	1,33E-03	12
PKHD1L1	4,29E-03	12
PEG3	6,03E-03	12
SLC39A12	3,01E-05	11
HEPH	4,44E-05	11
ZNF208	6,44E-05	11
NLRP14	1,29E-04	11
SPEF2	2,43E-04	11
MUC5B	5,73E-04	11
GRIN2B	7,46E-04	11
PTPRT	7,46E-04	11
AFF2	9,61E-04	11
COL12A1	3,63E-03	11
NLRP3	6,37E-03	11
NBEA	3,19E-05	10
KCNB2	3,13E-04	10
SALL1	4,31E-04	10
ABCB5	1,03E-03	10
SCN3A	1,34E-03	10
KCNT2	3,48E-03	10
HECW1	4,32E-03	10
KIAA1109	6,47E-03	10
CTNNA2	9,39E-03	10
SETBP1	9,39E-03	10

b

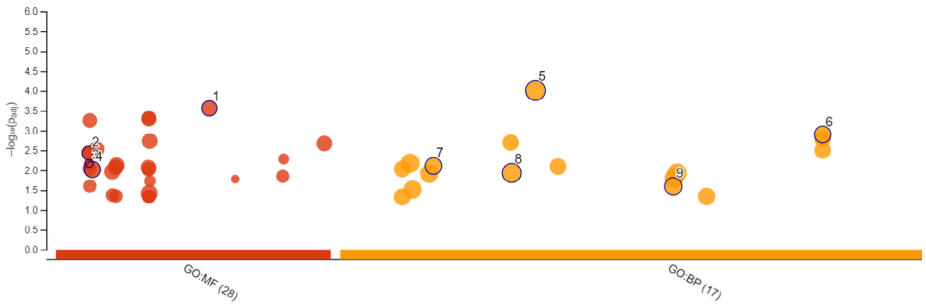

Source	Function	Term_id	Adjusted p_value	Genes
GO:MF	1. Metal ion transmembrane transporter activity	GO:0046873	2,75E-04	*RYR2; RYR3; HCN1; SLC39A12; GRIN2B; KCNB2; SCN3A; KCNT2*
GO:MF	2. Extracellular matrix structural constituent	GO:0005201	3,74E-03	*COL11A1; FBN2; COL3A1; VCAN; COL12A1*
GO:MF	3. Ryanodine-sensitive calcium-release channel activity	GO:0005219	6,70E-03	*RYR2; RYR3*
GO:MF	4. Calcium ion binding	GO:0005509	9,60E-03	*RYR2; SPTA1; PCDH15; FAT4; RYR3; FBN2; VCAN; CUBN*
GO:BP	5. Multicellular organismal process	GO:0032501	9,72E-05	*RYR2; USH2A; SPTA1; COL11A1; PCDH15; FAT4; RYR3; FBN2; COL3A1; VCAN; HCN1; CUBN; ADGRB3; PKHD1L1; SLC39A12; NLRP14; SPEF2; GRIN2B; AFF2; COL12A1; NLRP3; NBEA; KCNB2; SALL1; ABCB5; SCN3A; HECW1; CTNNA2*
GO:BP	6. Inorganic cation transmembrane transport	GO:0098662	1,25E-03	*RYR2; RYR3; HCN1; SLC39A12; HEPH; GRIN2B; KCNB2; SCN3A; KCNT2; HECW1*
GO:BP	7. Animal organ morphogenesis	GO:0009887	7,83E-03	*RYR2; COL11A1; PCDH15; FAT4; FBN2; COL3A1; HCN1; SPEF2; SALL1; CTNNA2*
GO:BP	8. Cell differentiation	GO:0030154	1,17E-02	*USH2A; SPTA1; COL11A1; PCDH15; FAT4; FBN2; COL3A1; VCAN; HCN1; ADGRB3; SLC39A12; NLRP14; SPEF2; COL12A1; NLRP3; SALL1; ABCB5; HECW1; CTNNA2*
GO:BP	9. Generation of neurons	GO:0048699	2,55E-02	*USH2A; PCDH15; FAT4; COL3A1; VCAN; HCN1; ADGRB3; SLC39A12; SALL1; HECW1; CTNNA2*

Fig. 3. Co-occurring mutational status of *SMARCA4* with all mutated genes in LUAD. (**A**) Mutated genes in LUAD patients showing co-occurrence with *SMARCA4*. The total number of samples is 565. (**B**) Functional enrichment analysis using the g.profiler web tool. We selected those functions that the software itself indicates as relevant to the function cluster GO molecular function, or GO biological processes.

For the thirty-one transcripts that were downregulated, we used the g.Profiler[14]. We obtained four distinct and statistically significant functions (GO biological process), all related to the immune system including "Antigen processing and presentation, endogenous lipid antigen via MHC class Ib" ($p = 4.154e-05$), "Regulation of leukocyte mediated cytotoxicity" ($p = 0.014$), "T-cell mediated immunity" ($p = 0.047$) and "Positive regulation of T cell mediated cytotoxicity" ($p = 0.036$). *CD1A, CD1E, CD1C, CX3CR1,* and *MYO1G* were the genes included in these functions (Fig. 4C). Other functions in different GO were detected (Supplementary table 3).

Association of the identified gene-set with immune populations in SMARCA4 non-altered tumors

As LUAD tumors with genomic alterations of *SMARCA4* had a downregulation of antigen processing via MHC class Ib genes including, *CD1A, CD1C, CD1E, CX3CR1,* and *MYO1G,* we aimed to explore the correlation of these genes with immune populations. The increase in expression of *CD1A, CD1C, CD1E, CX3CR1* and *MYO1G* showed a strong positive correlation with dendritic cells (DC) (Corr Rho 0.684; 0.761; 0.714; 0.525 and 0.440 respectively) and dendritic cells resting (DCR) (Corr Rho 0.744; 0.685; 0.692; 0.483 and 0.248 respectively), as displayed in Fig. 5A and B.

Association with clinical outcome and response to ICI of the identified gene set

We next aimed to evaluate the association of the identified set of genes in relation to clinical outcome and response to anti-PD(L)1.

As can be seen in Figs. 6 A and B, the increased expression of each gene signature resulted in a better prognosis in a set of patients with different tumors (including 90 bladders, 103 esophageal cancers, 28 glioblastomas, 22 hepatics, 110 head and neck cancers, 570 melanomas, 21 non-small cell lung cancers, 22 small cell lung cancer, and 348 urothelial cancers).

For both anti-PD-1 (Fig. 6A) and anti-PD-L1 treatments (Fig. 6B), the signature of these genes showed a favorable outcome. For treatments with anti-PD-1 (Fig. 6A) the best signature was the one formed by *CD1A, CD1E, CD1C,* and *MYO1G* (HR 0.48 CI 0.36–0.64, $p = 3.4e-07$). In the case of anti-PD-L1 (Fig. 6B), *CD1A, CD1E, CD1C, MYO1G,* and *CX3CR1* showed the best prognosis (HR 0.57 CI:0.44–0.73, $p = 9.2e-06$).

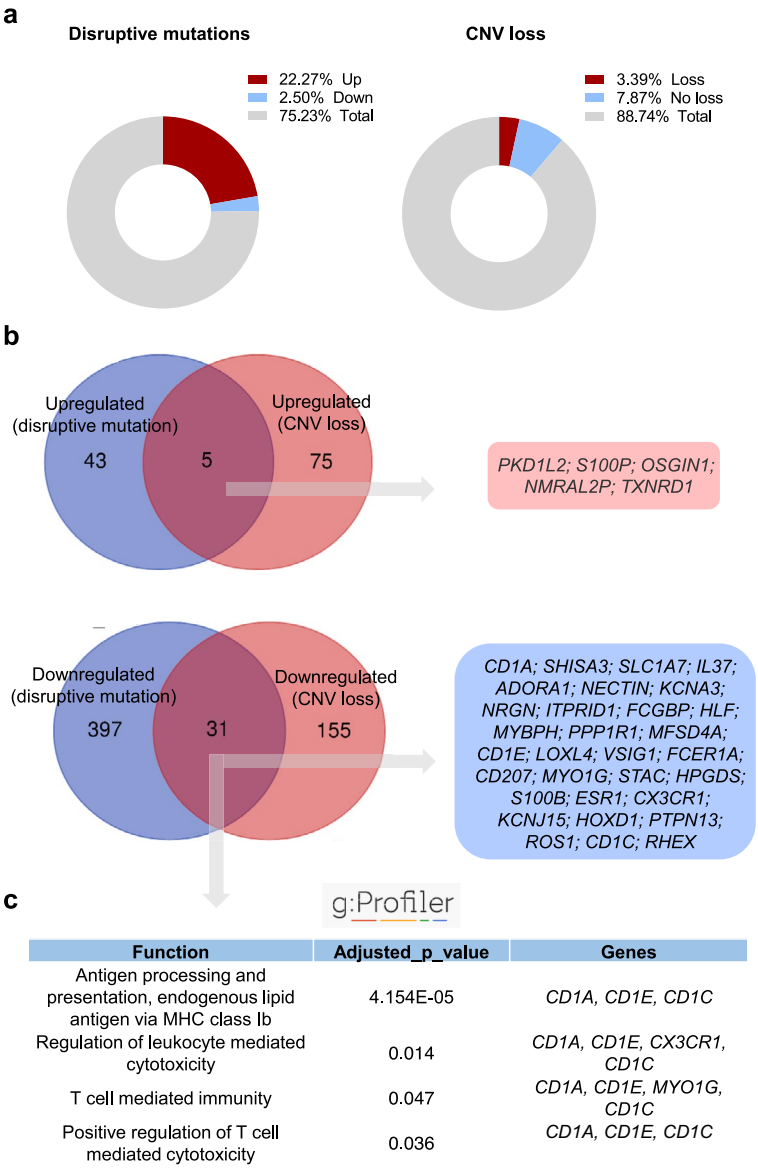

Function	Adjusted_p_value	Genes
Antigen processing and presentation, endogenous lipid antigen via MHC class Ib	4.154E-05	*CD1A, CD1E, CD1C*
Regulation of leukocyte mediated cytotoxicity	0.014	*CD1A, CD1E, CX3CR1, CD1C*
T cell mediated immunity	0.047	*CD1A, CD1E, MYO1G, CD1C*
Positive regulation of T cell mediated cytotoxicity	0.036	*CD1A, CD1E, CD1C*

Fig. 4. Transcriptomic profile of tumors with mutations or CNV loss. (**A**) Percentage of genes upregulated and downregulated when *SMARCA4* was altered or had CNV loss. (**B**) Venn diagram of common genes between those upregulated and downregulated with disruptive mutation and CNV loss of *SMARCA4*. (**C**) Functional enrichment analysis using the g.profiler web tool. We selected those functions that the software itself indicates as relevant to the function cluster GO molecular function, or GO biological processes.

Discussion

In the present article, we have evaluated the genomic, transcriptomic, and immunologic profile of NSCLC tumors with mutations or deletions at *SMARCA4*. Identification of subgroups of patients with specific molecular alterations that could benefit from a particular target agent is key in oncology, to improve efficacy and maintain an adequate safety profile. In this regard, strategies aiming to target *SMARCA4* mutated tumors are currently in clinical development[6].

In addition, evaluation of the immunologic profile of this family of agents could help to select combinational strategies to be implemented in the future. In this context, some genomic alterations in NSCLC are linked with a particular immunologic profile as is the case for mutations at the *EGFR* or *K-RAS* gene[15–17]. In this context, little evidence exists regarding the transcriptomic and immunologic profile of NSCLC tumors with molecular alterations at *SMARCA4*.

In our study, we first evaluated the frequency of *SMARCA4* genomic alterations by mapping publicly available datasets. We first observed that other tumor types, beyond NSCLC, expressed a higher proportion of *SMARCA4* genomic alterations, including endometrial, melanoma, esophageal, or ovarian. Among the NSCLC types, the proportion in LUAD was higher than in LUSC. In LUAD, most of the alterations were disruptive mutations compared with gene deletions or structural variants. Similarly, disruptive mutations were more frequently

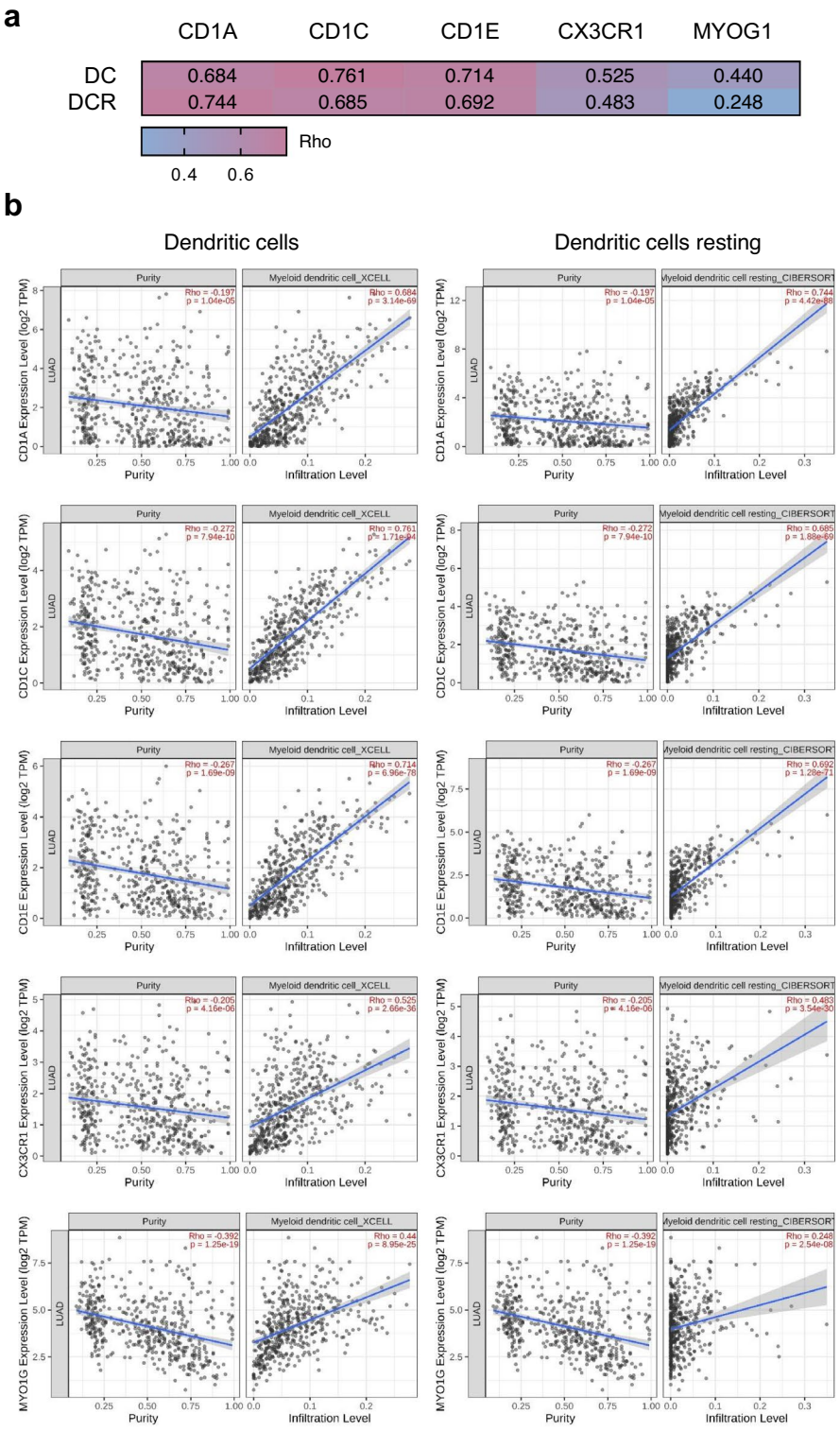

Fig. 5. Immunologic correlation of downregulated genes with myeloid dendritic cells. (**A**) Heatmap of Rho value correlation of *CD1A, CD1C, CD1E, CX3CR1,* and *MYO1G* genes with dendritic cells in LUAD. (**B**) Dot plot showing the expression in LUAD (n = 515) of downregulated genes *(CD1A, CD1C, CD1E, CX3CR1,* and *MYO1G*) in the Y axes and the infiltration level of some immune cells (myeloid dendritic cells and dendritic cells resting) in the X axes. The blue regression line shows the positive correlation, and Rho, and Spearman's p-value data are presented in red.

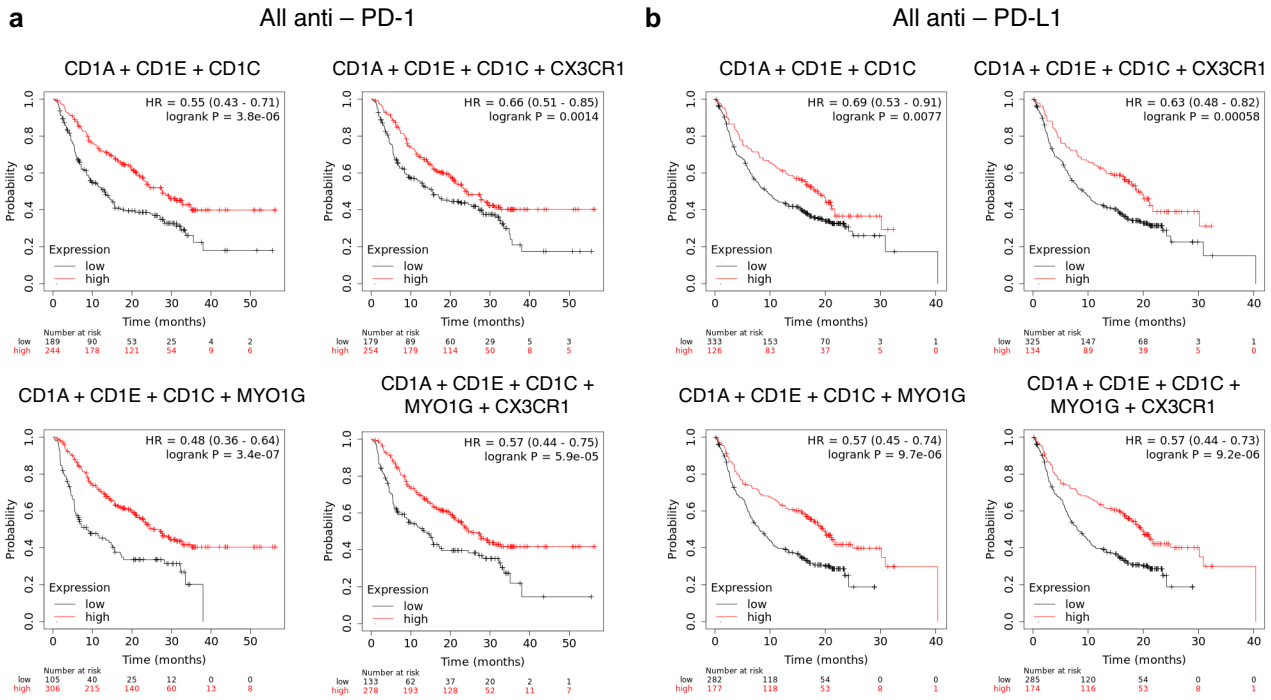

Fig. 6. Clinical outcome analysis of *CD1A, CD1C, CD1E, CX3CR1,* and *MYO1G* immune gene-set combination in each stage of HNSCC patients. Survival plots of the combination of each functional group of immune genes in patients with several tumors (90 bladder, 103 esophageal cancers, 28 glioblastomas, 22 hepatics, 110 head and neck cancers, 570 melanomas, 21 non-small cell lung cancers, 22 small cell lung cancer, and 348 urothelial cancers) with (**A**) anti-PD1 and (**B**) anti-PD-L1treatments. Patients whose tumors harbor high gene expression levels predicted better survival (red line), and those with low gene expression levels predicted worse survival (black line). The number of patients at risk at every time (months), with high (in red) and low gene expression (in black) are displayed. HR for risk of death and OS are displayed. The gene combination is displayed at the top of the figure.

present in LUSC. Finally, in both groups, truncating mutations were the most frequent alteration within the group. This data highlights the importance of this alteration in NSCLC, particularly in LUAD, but also the relevant prevalence in other solid tumors.

Although the study by Yumeng Tian et al. found that *SMARCA4, KRAS* and *TP53* showed co-occurrence in a large percentage of patients[6], in our analysis with CBioportal (TCGA-PanCancer atlas), these genes do not show significant co-occurrence (Supplementary Fig. 2).

Functions associated with our co-occurring mutated genes included calcium-related pathways, response to mechanical stimuli, or adhesion, among others. The functions identified suggest the relevant role in the regulation of transcription by altering the chromatin structure[6].

When evaluating the transcriptomic profile associated with genomic alterations of *SMARCA4,* we observed that most of the modified genes were downregulated; which aligns with the role of *SMARCA4* in the regulation of transcription[6]. Indeed, commonly and shared down-regulated genes included a total of thirty-one. From those genes within this group, enriched biological functions included: antigen processing and presentation, endogenous lipid antigen via MHC class Ib", "Regulation of leukocyte mediated cytotoxicity" or "T-cell mediated immunity". This was an unexpected observation that involved genes like *CD1C, CXC3CR1, CD1A, CD1E* and *MYO1G*. Therefore, genomic alterations in *SMARCA4* negatively modify the antigen presentation process. Indeed *CD1C, CD1A,* and *CD1E* are structurally related to the major histocompatibility complex (MHC) proteins, and they form heterodimers with beta-2-microglobulin[18]. The CD1 proteins mediate the presentation of primarily lipid and glycolipid antigens of self or microbial origin to T cells[18]. CXC3CR1 is a transmembrane protein and chemokine involved in the adhesion and migration of leukocytes[19]. MYO1G is a plasma membrane-associated class I myosin that is abundant in T and B lymphocytes and mast cells[20]. MYO1G acts as a regulator of T-cell migration by generating membrane tension, enforcing cell-intrinsic meandering search, thereby enhancing the detection of rare antigens during lymph node surveillance, and enabling pathogen eradication[21].

When we explored the association of the identified gene signature with response to anti-PD-(L)1 therapy, we observed that this set of genes predicted clinical activity to this type of agents. Combinations of different set genes predicted better progression-free survival (PFS) and overall survival (OS). Of note, other mutations have been associated with a lack of response to ICI including *KEAP1, STK11,* or *PBRM1*[22]. In a recent study, there was no difference in outcome (PFS or OS) on ICIs by *SMARCA4* alteration status, although differences in responses were detected and the benefit was higher in patients treated with ICI versus those with chemotherapy[7]. Sporadic cases have also reported this association[23,24]. On the other hand, another study showed a different result

suggesting that *SMARCA4* mutations predicted lack of efficacy to anti PD1 agents[5]. In this study *SMARCA4* loss in tumor cells led to profound downregulation of STING, IL1β and other components of the innate immune system[5]. This data aligns with our observation of a downregulation of antigen presenting genes.

We acknowledge the limitations of this work. Our article is based on bio-informatic information generated using publicly available datasets, therefore this data can be considered as hypothesis-generating. In addition, the data used in this work did not contain information regarding clinical activity of check-point inhibitors so further studies should be performed to confirm the reported findings.

Conclusions

Our study explores the transcriptomic profile of tumors with genomic alterations of *SMARCA4* identifying a downregulation of relevant genes involved in the activation of T cells through antigen presentation within dendritic cells. This data could suggest that tumors with lack of *SMARCA4* would have less clinical activity to anti PD1 therapies. However, to confirm these observations further prospective studies are needed.

Data availability

The data generated or analyzed during the current study are included in this published article [and its supplementary information files].

Received: 24 April 2024; Accepted: 13 May 2025
Published online: 22 May 2025

References

1. Zhang, Z. et al. Integrated analysis of single-cell and bulk RNA sequencing data reveals a pan-cancer stemness signature predicting immunotherapy response. *Genome Med.* **14**, 1–18 (2022).
2. Blons, H., Garinet, S., Laurent-Puig, P. & Oudart, J. B. Molecular markers and prediction of response to immunotherapy in non-small cell lung cancer, an update. *J. Thorac. Dis.* **11**, S25–S36 (2019).
3. Morafraile, E. C. et al. Mapping immune correlates and surfaceome genes in BRAF mutated colorectal cancers. *Curr. Oncol.* **30**, 2569–2581 (2023).
4. Memmott, R. M., Wolfe, A. R., Carbone, D. P. & Williams, T. M. Predictors of response, progression-free survival, and overall survival in patients with lung cancer treated with immune checkpoint inhibitors. *J. Thorac. Oncol.* **16**, 1086–1098 (2021).
5. Wang, Y. *et al.* SMARCA4 mutation induces tumor cell-intrinsic defects in enhancer landscape and resistance to immunotherapy. *bioRxiv* 2024.06.18.599431 (2024) https://doi.org/10.1101/2024.06.18.599431.
6. Tian, Y., Xu, L., Li, X., Li, H. & Zhao, M. SMARCA4: Current status and future perspectives in non-small-cell lung cancer. *Cancer Lett.* **554**, 216022 (2023).
7. Schoenfeld, A. J. et al. The genomic landscape of SMARCA4 alterations and associations with outcomes in patients with lung cancer. *Clin. Cancer Res.* **26**, 5701–5708 (2021).
8. Nicholson, A. G. et al. The 2021 WHO classification of lung tumors: Impact of advances since 2015. *J. Thorac. Oncol.* **17**, 362–387 (2022).
9. Cerami, E. et al. The cBio cancer genomics portal: An open platform for exploring multidimensional cancer genomics data. *Cancer Discov.* **2**, 401–404 (2012).
10. Li, T. et al. TIMER2.0 for analysis of tumor-infiltrating immune cells. *Nucl. Acids Res.* **48**, W509–W514 (2020).
11. Lánczky, A. & Győrffy, B. Web-based survival analysis tool tailored for medical research (KMplot): Development and implementation. *J. Med. Internet Res.* **23**, e27633 (2021).
12. Kovács, S. A., Fekete, J. T. & Győrffy, B. Predictive biomarkers of immunotherapy response with pharmacological applications in solid tumors. *Acta Pharmacol. Sin.* **44**, 1879–1889 (2023).
13. Stelzer, G. et al. The GeneCards suite: From gene data mining to disease genome sequence analyses. *Curr. Protoc. Bioinforma.* **54**, 1.30.1-1.30.33 (2016).
14. Kolberg, L. et al. g:Profiler—interoperable web service for functional enrichment analysis and gene identifier mapping (2023 update). *Nucl. Acids Res.* **51**, W207–W212 (2023).
15. Alcaraz-Sanabria, A. et al. Transcriptomic mapping of non-small cell lung cancer K-RAS p.G12C mutated tumors: Identification of surfaceome targets and immunologic correlates. *Front. Immunol.* **12**, 5337 (2022).
16. Cao, X. et al. Granzyme B and perforin are important for regulatory T cell-mediated suppression of tumor clearance. *Immunity* **27**, 635–646 (2007).
17. Kapoor, S. S. & Zaiss, D. M. W. Emerging role of EGFR mutations in creating an immune suppressive tumour microenvironment. *Biomedicines* **10**, 52 (2021).
18. Brigl, M. & Brenner, M. B. CD1: Antigen presentation and T cell function. *Annu. Rev. Immunol.* **22**, 817–890 (2004).
19. Lu, X. Structure and function of ligand CX3CL1 and its receptor CX3CR1 in cancer. *Curr. Med. Chem.* **29**, 6228–6246 (2022).
20. Pierce, R. A. et al. The HA-2 minor histocompatibility antigen is derived from a diallelic gene encoding a novel human class I myosin protein. *J. Immunol.* **167**, 3223–3230 (2001).
21. Stein, J. V. T cell motility as modulator of interactions with dendritic cells. *Front. Immunol.* **6**, 164876 (2015).
22. La Fleur, L. et al. Mutation patterns in a population-based non-small cell lung cancer cohort and prognostic impact of concomitant mutations in KRAS and TP53 or STK11. *Lung Cancer* **130**, 50–58 (2019).
23. Naito, T. et al. Successful treatment with nivolumab for SMARCA4-deficient non-small cell lung carcinoma with a high tumor mutation burden: A case report. *Thorac. Cancer* **10**, 1285–1288 (2019).
24. Henon, C. et al. Long lasting major response to pembrolizumab in a thoracic malignant rhabdoid-like SMARCA4-deficient tumor. *Ann. Oncol.* **30**, 1401–1403 (2019).

Acknowledgements

This project was supported by the National Research, Development, and Innovation Office of Hungary (PharmaLab, RRF-2.3.1-21-2022-00015 and TKP2021-NVA-15).

Author contributions

C.N.J.—Investigation; Methodology; Visualization; Writing–original draft. E.G.L.—Investigation; Writing–review & editing. C.D.T., L.P.H., A.S. – Validation; Visualization; Writing–review & editing. B.G., G.M. – Software; Writing–review & editing. B.D., I.M., M.P., J.B., A.M., P.P.S., E.C., V.M.—Writing–review & editing. A.O. Con-

ceptualization; Writing–original draft; Funding acquisition.

Funding
These results have been supported by Instituto de Salud Carlos III (PI19/00808), ACEPAIN, Diputación de Albacete, CIBERONC, and CRIS Cancer Foundation (to A.O.). The work carried out in our laboratories receives support from the European Community through the Regional Development Funding Program (FEDER).

Declarations

Competing interests
A.O. is currently a consultant for NMS outside the current work and consultant services for Servier, Worldwide International Trials and CancerAppy. Former employee of Symphogen. No conflict of interest to declare in relation to this manuscript. V.M. reports personal fees from Bristol-Myers Squibb, Bayer, Janssen, and Pieris outside the submitted work. E.C. reports grants and personal fees from Astellas, Novartis, Nanobiotix, Pfizer, Janssen-Cilag, PsiOxus Therapeutics, Merck, BristolMyers Squibb, Seattle Genetics, Boehringer Ingelheim, AstraZeneca, Roche/Genentech, Servier, Celgene, AbbVie, Amcure, Alkermes, PharmaMar, and BeiGene, outside the submitted work. P.P. reports grant/research support from Bristol-Myers Squibb, AstraZeneca, and MSD, outside the submitted work. The other authors declare that they have no competing interests.

Additional information
Supplementary Information The online version contains supplementary material available at https://doi.org/10.1038/s41598-025-02494-x.

Correspondence and requests for materials should be addressed to A.O.